

Effect of Hexafluoroisopropylidene on Perfluorocyclobutyl Aryl Ether Copolymer Solution Behavior in Supercritical CO₂ and Propane

Jun Liu,[†] Bryan K. Spraul,[‡] Chris Topping,[‡] Dennis W. Smith, Jr.,[‡] and Mark A. McHugh^{*,†}

Department of Chemical and Life Science Engineering, Virginia Commonwealth University, Richmond, Virginia 23284, and Department of Chemistry and Center for Optical Materials Science and Engineering Technologies, Advanced Materials Research Laboratory (AMRL), Clemson University, Clemson, South Carolina 29634-0973

Received March 1, 2007; Revised Manuscript Received June 7, 2007

ABSTRACT: High-pressure phase behavior data reported here demonstrate the nuanced impact fluorine exerts on polymer solubility in supercritical fluid solvents. Copolymers are used that contain a perfluorocyclobutyl ether group with varying amounts of bis-aryl isopropylidene (**6H**) or bis-aryl hexafluoroisopropylidene (**6F**). Surprisingly, it takes at least 2000 bar and 190 °C to dissolve the **6H** homopolymer in CO₂ even though every repeat group has ~15 mol % fluorine and two ether oxygens, both of which enhance polymer solubility in CO₂. The copolymer cloud-point curves in CO₂ monotonically shift significantly to lower temperatures and pressures as the **6F** content is increased from 0 to 100%. This shift is ascribed to the decrease in long-range, chain–chain interactions due to poor packing of the **6F**-rich chains, to the increase in solvent accessible surface area of fluorinated groups, and to the increase in the fractional free volume (FFV) of **6F**-rich chains. The cloud-point curves in propane also initially shift to lower temperatures and pressures with increasing **6F** content, but the **6F** homopolymer and **6H** homopolymer curves cross one another so that the **6H** homopolymers are more soluble at low temperatures while **6F** homopolymers are more soluble at high temperatures. The reversal in propane solubility behavior with increasing **6F** content and temperature results from a delicate balance between repulsive fluorine–hydrocarbon interactions that do not favor copolymer solubility and reduced long-range, chain–chain interactions and increased copolymer FFV that both favor copolymer solubility. The cloud-point data also show that for both CO₂ and propane the impact of **6F** content is greater than the impact of weight-average molecular weight in the range 15–93 kg/mol, where molecular weight is expected to have a large impact.

Introduction

Supercritical fluids (SCF) solvents, especially CO₂, have been widely applied in many different fields, such as extractions,¹ reactions,^{2–5} and material preparation and processing.^{6–9} The solubility of a given substance in an SCF solvent is a key factor affecting the application of these interesting solvents. Most polymers, with the exception of certain semifluorinated or silicone-containing amorphous polymers, are insoluble in CO₂ unless extreme temperatures or pressures are used.¹ Since SCF solvents are weak solvents, small alterations to polymer architecture can significantly affect the conditions needed to dissolve a given polymer in an SCF solvent. For example, poly(vinyl acetate) (PVAc) and poly(methyl acrylate) have similar structures, but PVAc dissolves in CO₂ at much lower pressures likely due to the easier accessibility of CO₂ to the carbonyl group in PVAc.^{10,11} Changes in polymer backbone architecture can also moderate the strength of chain–chain interactions that depend on the ability of the polymer chains to pack in solution.

Although it is now well-known that fluorinating a polymer enhances its solubility in CO₂, there still remains contradictory evidence on the existence of a specific interaction between CO₂ and a fully fluorinated molecule. Certain NMR results suggested there is no specific interaction between fluorine and CO₂^{12,13} while other studies suggested just the opposite.^{14–16} Molecular

modeling studies have also proposed both possibilities.^{17–26} For example, Stone et al.²⁵ demonstrated that CO₂ and perfluorocarbons do not exhibit any substantial specific interaction which is consistent with the results of other modeling studies^{17–20,24} and phase behavior studies of fluorinated polymer–CO₂ mixtures.^{27,28} Conversely, Fried and Hu²¹ concluded that a favorable polar interaction does exist between CO₂ and nonpolar CF₄ although they also concluded that a favorable interaction exists for CO₂ with semifluorinated hydrocarbons, which, in our opinion, is more likely given that semifluorinated hydrocarbons possess a polar moment. Several of the modeling studies^{17,24,25} demonstrated that enhanced interactions, leading to improved solubility, are realized with semifluorinated materials having both Lewis acid and base sites configured in a manner to allow both sites to interact simultaneously. Interestingly, one study²² proposed that enhanced interactions between fluorine and CO₂ resulted from the increased solvent accessible surface of a fluorinated aromatic solute rather than from a specific CO₂–fluorine interaction.

In the present study we investigate the effect of fluorination on the solubility of perfluorocyclobutyl (PFCB) aryl ether copolymers in CO₂ and in nonpolar propane. These copolymers contain a PFCB ether group with a bis-aryl isopropylidene (**6H**) or a bis-aryl hexafluoroisopropylidene (**6F**) group. Scheme 1 shows the thermal cycloaddition polymerization route to synthesize the PFCB copolymers. Upon heating, the trifluorovinyl ethers groups cyclodimerize to form PFCB linkages between aromatic spacers. Copolymers with different **6F** content are synthesized by controlling the **6H**:**6F** starting ratio. The **6F**

* To whom correspondence should be addressed: E-mail: mmchugh@vcu.edu.

[†] Virginia Commonwealth University.

[‡] Clemson University.

Scheme 1. Thermal Cycloaddition Polymerization Route To Synthesize the PFCB Copolymers from 2,2-Bis(4-trifluorovinylphenoxy)propane (6H**) and 2,2-Bis(4-trifluorovinylphenoxy)-1,1,1,3,3,3-hexafluoropropane (**6F**)**

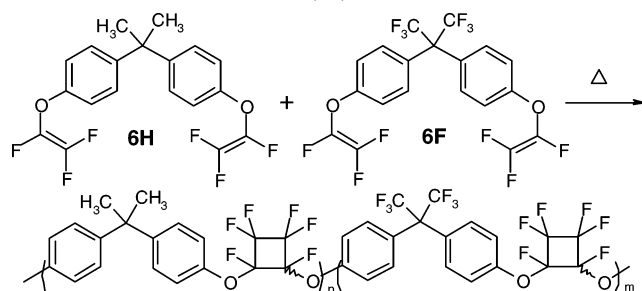


Table 1. Physical Properties of the Solvents Used in This Study

	T_c^a (°C)	P_c^b (bar)	α^c 10^{-24} cm^3	μ^d (D)	Q^e (10^{-26} erg $^{1/2}$ $\text{cm}^{5/2}$)
CO ₂	31.0	73.8	2.65	0	-4.3
propane	96.7	42.5	6.26	0.1	0

^a Critical temperature. ^b Critical pressure. ^c Polarizability. ^d Dipole moment. ^e Quadrupole moment.

group enhances polymer solubility in common solvents, improves thermal and thermal oxidative stability, lowers the dielectric constant, increases moisture resistance, imparts optical transparency, and improves resistance to UV radiation.^{29,30} It is also important to note that the CF₃ group exhibits a steric effect similar to that of an isopropyl hydrocarbon group,³¹ which also increases the free volume of the polymer.³² Our earlier phase behavior studies show that CO₂ does not have any significant specific interaction with CF₂ or CF₃ in a nonpolar, polymer repeat group.²⁸ Therefore, the addition of the two trifluoromethyl groups in **6F** is not expected to increase copolymer solubility in CO₂ solely due to enhanced favorable intermolecular interactions, given that the **6H** homopolymer already has a fluorine content of 14.6 mol % due to the polar, PFCB ether groups. The work presented here presents further evidence from an earlier study³³ suggesting that the steric hindrance from the **6F** trifluoromethyl groups minimizes conformation-dependent chain–chain interactions and reduces longer-range interactions similar to those found with polymers that form liquid crystals.

Table 1 lists the critical temperatures and pressures, polarizability, dipole moment, and quadrupole moment of the two solvents used in this study. Propane is a nonpolar SCF solvent with a larger polarizability than CO₂, which means that propane should be a better solvent than CO₂ for the copolymers with a high **6H** content. Neither solvent exhibits a dipole moment although CO₂ does have a quadrupole moment which suggests that CO₂ will be a better solvent than propane for the copolymers with a high **6F** content.

Experimental Section

Materials. 2,2-Bis(4-hydroxyphenyl)hexafluoropropane was purchased from Oakwood Chemicals, 2,2-bis(4-hydroxyphenyl)propane was purchased from Acros, medical grade CO₂ was purchased from Roberts Oxygen, and propane (98%) was obtained from Aldrich. All of these chemicals were used as received. Trifluorovinyl ether monomers are commercially available from Tetramer Technologies, LLC (Pendleton, SC, www.tetramertechnologies.com) and distributed by Oakwood Chemicals, Inc. (Columbia, SC).

Polymer Synthesis. The monomers 2,2-bis(4-trifluorovinylphenoxy)-1,1,1,3,3,3-hexafluoropropane (Scheme 1, **6F**) and 2,2-

Table 2. Physical Properties of the Polymers Used in This Study

	6F (wt %) ^a	6F (mol %) ^b	fluorine (mol %) ^c	M_w^d (kg mol ⁻¹)	M_w/M_n	T_g^e (°C)
6H_H	0	0	14.6	93.0	3.2	102
6H_L	0	0	14.6	15.6	2.0	66
6F₂₁	25	20.7	17.7	68.0	2.8	103
6F₄₄	50	43.9	21.1	38.1	2.4	104
6F₇₀	75	70.1	24.9	20.5	1.7	103
6F_H	100	100.0	29.3	62.6	2.0	113
6F_L	100	100.0	29.3	13.7	1.6	103

^a Weight percent of **6F** in the starting reaction mixture. ^b Mole percent of **6F** in the starting reaction mixture. ^c Mole percent of fluorine atoms in the starting reaction mixture. ^d Weight-average molecular weight. ^e Glass transition temperature.

bis(4-trifluorovinylphenoxy)propane (Scheme 1, **6H**) were synthesized from 2,2-bis(4-hydroxyphenyl)hexafluoropropane and 2,2-bis(4-hydroxyphenyl)propane, respectively, using a technique described by Smith, Jr., et al.³⁴ The polymers were subsequently synthesized by thermal cycloaddition reaction of the comonomers, as shown in Scheme 1.³⁴ Typically, monomers were added to 30 mL ampules that were sealed under vacuum and immersed in an oil bath at 180 °C for 48 h. The bath temperature was then increased to 200 °C for 12 h and increased further still to 230 °C for an additional 3 h. The ampules were removed from the bath and allowed to cool. The resultant polymers were dissolved in a minimum amount of dichloromethane and precipitated into methanol. The precipitate was dried and characterized using ¹⁹F NMR. Differential scanning calorimetry was performed on a TA Q1000 to determine the glass transition temperature, and gel permeation chromatography (GPC) was used to determine the molecular weights and molecular weight distributions of the polymer samples using polystyrene as a reference.

Phase Behavior Measurements. The apparatus and techniques used to obtain polymer–supercritical fluid cloud-point curves are described elsewhere.²⁸ The main component of the experimental apparatus is a variable-volume high-pressure cell, made of nitronic 50 stainless steel with an outside diameter of 6.35 cm, an inside diameter of 1.6 cm, and ~15 cm³ working volume. The cell was first loaded with a measured amount of polymer, and entrapped air is removed from the cell by flushing the cell several times with propane or CO₂ at pressures of ~3 bar. Gaseous propane or CO₂ was added to the cell gravimetrically to within ±0.05 g using a high-pressure bomb. The mixture in the cell was viewed with a borescope (Olympus Corp., model F100-024-000-55) placed against a sapphire window secured at one end of the cell. The cell contents were mixed using a magnetic stir bar activated by an external magnet. The solution temperature was measured to within ±0.1 °C (type K thermocouple calibrated against a NIST certified thermometer) and held to within ±0.5 °C. The system pressure was measured using a transducer (Viatran model 245 accurate to within ±3.4 bar). The mixture in the cell was compressed isothermally to a single phase, and then the pressure was slowly reduced until a second phase appeared. The reported cloud point is the midpoint between the pressure where the clear solution just starts to become hazy and the pressure where the solution becomes so cloudy that the stir bar is obscured. This clear-to-cloudy pressure transition was between 20 and 100 bar. The reported cloud-point pressure is an average of at least three repetitive cloud-point measurements.

Results and Discussion

Scheme 1 shows the structure of the statistically random copolymers synthesized for this study. The **6H** monomer has six hydrogens on the isopropylidene group which are replaced with six fluorine atoms in **6F**. Table 2 lists the physical properties of the resulting polymers used in this study. Copolymers with 0, 21, 44, 70, and 100 mol % **6F** are synthesized by controlling the relative concentrations of the two different

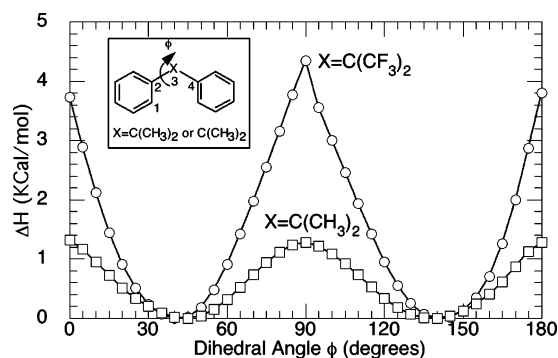


Figure 1. Energy barrier for benzene ring rotation determined for isopropylidene diphenyl and hexafluoroisopropylidene diphenyl using the MOPAC PM5 method with Fujitsu CAChe 4.9 software.

monomers in the feed mixture that, upon heating, react via cyclodimerization of the trifluorovinyl ether monomers. The ^{19}F NMR and refractive index data show that the final monomer composition in the polymer was the same as the feed monomer ratio for all the polymers.³⁵ Note that the fluorine content of these polymers varies between 14.6 and 29.3 mol % since each repeat group contains a PFCB ether group.

The incorporation of the **6F** group in the chain backbone should increase the free volume and the T_g of the resultant polymer since the steric effect of the two CF_3 groups further inhibits free rotation of an already stiff polymer backbone.^{29,30,32,36} To provide insight into the impact of **6F** on chain torsional mobility, semiempirical quantum mechanics calculations were performed for two model compounds, isopropylidene diphenyl and hexafluoroisopropylidene diphenyl, using the MOPAC PM5 method³⁷ with CAChe 4.9 software. Figure 1 presents the results of energy barrier calculations at 5° increments of the dihedral angle ϕ for $\text{X} = \text{C}(\text{CH}_3)_2$ and $\text{C}(\text{CF}_3)_2$. The maximum rotational barrier was ~ 4.35 kcal/mol for $\text{C}(\text{CF}_3)_2$ and only ~ 1.33 kcal/mol for $\text{C}(\text{CH}_3)_2$, similar to results from previous studies.³² Hence, chains rich in **6F** should have higher T_g s and should pack less efficiently leading to higher fractional free volume (FFV).³²

However, the T_g s of the PFCB copolymers used in this study are all close to 103°C , with the exceptions of **6H_L** and **6F_H**. T_g does not change as the fluorine content increases and the molecular weight decreases from **6F₂₁** to **6F₇₀**, which reflects the balance between the impact of **6F** on polymer conformation and the impact of molecular weight on the physical properties of the polymer. The T_g differences between **6H_H** and **6H_L** and between **6F_H** and **6F_L** are likely due to the differences in molecular weights for these sets of polymers. The impact of **6F** on T_g is most apparent by comparing **6H_L** and **6F_L**, both of which have similar molecular weights, but the T_g of **6H_L** is $\sim 35^\circ\text{C}$ lower than that of **6F_L**.

Figure 2 shows the significant impact of **6F** substitution on the solubility of the PFCB copolymers in supercritical CO_2 . It is worth noting that temperatures in excess of $\sim 165^\circ\text{C}$ and pressures in excess of 1600 bar are needed to dissolve PFCB homopolymers with 100 mol % **6H** groups even though each repeat group contains ~ 15 mol % fluorine plus two ether groups, which, in combination, enhance polymer solubility in CO_2 . Apparently, chain–chain interactions are stronger than PFCB– CO_2 cross-interactions for the **6H**-rich copolymers. As the amount of **6F** is increased to 100 mol %, the cloud-point curves in CO_2 shift to pressures as low as ~ 700 bar and temperatures of 20°C . We expect the configuration of the copolymer backbone to rearrange to accommodate the steric effect of CF_3 so that **6F**-rich chains do not allow for the facile packing needed

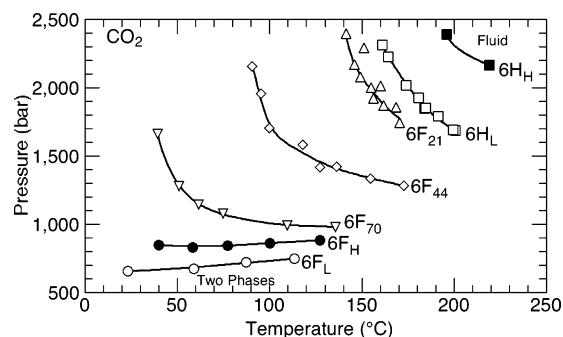


Figure 2. Impact of **6F** comonomer on the conditions needed to dissolve perfluorocyclobutyl aryl ether copolymers in supercritical CO_2 . The copolymer composition next to each curve is found in Table 2.

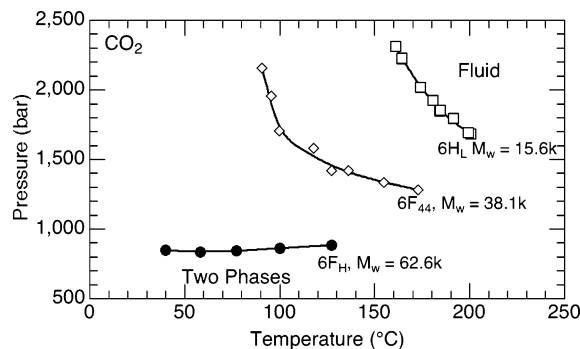


Figure 3. Impact of **6F** comonomer relative to polymer molecular weight, M_w , on the location of PFCB copolymers in supercritical CO_2 . The composition and M_w for each copolymer next to each curve is found in Table 2.

to promote long-range, chain–chain interactions. In addition, the molecular modeling results of Galand and Wipff²² suggest that chains rich in **6F** will configure in a manner that increases the solvent accessible surface area of fluorinated groups and, therefore, increases the amount of fluorine– CO_2 polar interactions found with semifluorinated polymers.^{17,21,27,28} As the temperature is reduced, the **6H_H** through **6F₇₀** curves exhibit a relatively sharp pressure increase that is typically associated with an energetic mismatch between polymer– CO_2 interactions relative to either polymer–polymer or CO_2 – CO_2 interactions that become exacerbated at “low” temperatures.²⁷ We expect that the **6F** curves would also exhibit an increase in pressure if the temperature is reduced sufficiently. It should also be noted that as **6F** is added to the polymer backbone, the FFV increases due to the inhibition of the free rotation of the polymer backbone. For example, Shimazu et al.³⁸ report a 10% increase in the FFV of a polyimide as **6F** is added to the polymer, and Espeso et al.³² report a 30% increase in FFV of a polyamide. An increase in the polymer FFV improves the likelihood of dissolving the polymer in a high-free-volume SCF solvent, such as CO_2 .

Inspection of the cloud-point curves in Figure 2 along with their respective molecular weights, M_w , in Table 2 indicates that the location of these curves is a stronger function of **6F** content than M_w , which is especially apparent when comparing the larger difference between the locations of the **6H_H** and **6H_L** curves relative to the **6F_H** and **6F_L** curves. Figure 3 shows that, at a fixed pressure, the cloud-point curves with the lower M_w are at higher, not lower, temperatures, which is behavior exactly opposite than expected had the dominant effect been the polymer M_w . Likewise, at a fixed temperature, the cloud-point pressures for the three curves in Figure 3 again are in the opposite order with respect to M_w . Shen et al. observed similar trends in the

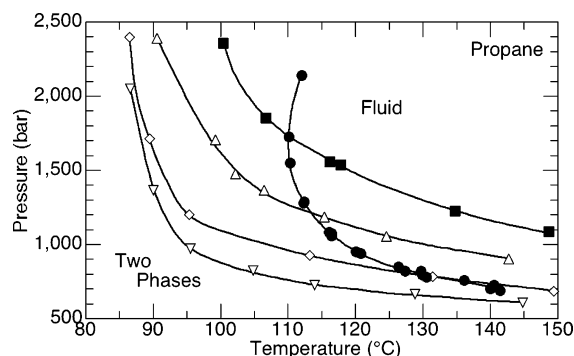


Figure 4. Impact of **6F** comonomer on the conditions needed to dissolve perfluorocyclobutyl aryl ether copolymers in supercritical propane. Not all of the cloud-point curves are shown here to avoid cluttering the graph. Filled squares, **6H_H**; open triangles, **6F₂₁**; open diamonds, **6F₄₄**; upside-down triangles, **6F₇₀**; filled circles, **6F_H**.

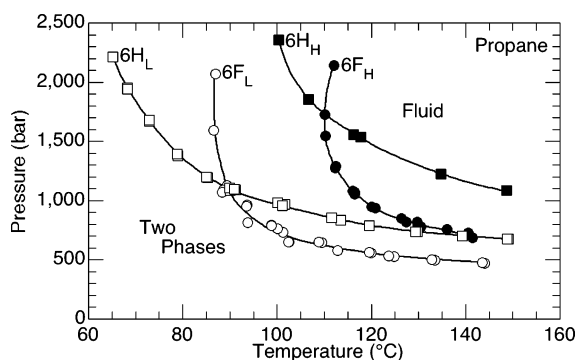


Figure 5. Comparison of the effect of molecular weight and **6F** content on the cloud-point curves for the **6H** and **6F** PFCB homopolymers in supercritical propane.

differences in the cloud-point curve characteristics of a **6H** and a **6F** lactide-based terpolymer, although in the Shen study the solvent was supercritical dimethyl ether.³³

Figure 4 shows the PFCB copolymer cloud-point curves in propane. Since alkyl fluorocarbons and hydrocarbons do not normally mix, we expect the copolymer chains to configure in a manner to minimize PFCB–propane interactions. Evidently, there is sufficient hydrocarbon content in the **6H_H** chain to promote dissolution in nonpolar propane, which has a higher polarizability than CO₂. Hence, the **6H_H**–propane cloud-point curve is at much lower temperatures and pressures than the **6H_H**–CO₂ curve. As the **6F** content in the PFCB copolymer is increased from 0 to 70 mol %, the cloud-point curves shift to lower temperatures and pressures, which also suggests that the reduction in long-range, chain–chain interactions dominates the effect of repulsive CF₃–propane interactions. Ultimately all of the cloud-point curves exhibit a sharp increase in pressure as the temperature is lowered, similar to the shapes of the CO₂

cloud-point curves. The shapes of the cloud-point curves in Figure 4 are characteristic of a mixture of a nonpolar and a polar component, and the temperature-dependent change in slope of the curve suggests the strong influence of unfavorable alkyl fluorocarbon–hydrocarbon interactions.^{27,39} The impact of fluorine on polymer solubility in a hydrocarbon is evident with the location of the **6F_H** curve that is at fairly low pressures at temperatures in excess of 130 °C but eventually exhibits an abrupt increase in pressure at temperatures higher than those where the break occurs with the **6F₂₁**, **6F₄₄**, and **6F₇₀** curves. Also, as previously mentioned, **6F** added to the polymer backbone increases the FFV due to the inhibition of the free rotation of the polymer backbone. Any increase in polymer FFV improves the likelihood of dissolving the polymer in a high-free-volume SCF solvent.

Figure 5 compares the cloud-point curves for the **6F** and **6H** homopolymers with equivalent molecular weight. The **6H** homopolymers were expected to be more soluble in propane than the **6F** homopolymers. However, at high temperatures the **6F** homopolymers dissolve in propane at lower pressures than the **6H** homopolymers likely because the steric effect of **6F** effectively reduces long-range chain–chain interactions as well as increases the free volume of the polymer. Other researchers have shown that the inclusion of the **6F** group in the polymer backbone generally improves polymer solubility.²⁹ For example, increases in solubility are observed for poly(ether ketone),³⁶ polyamides,⁴⁰ polyesters,⁴⁰ poly(aryl ether ketones),⁴¹ and poly(*p*-propylene)⁴² in typical organic liquid solvents when **6H** groups are replaced with **6F** groups. As the temperature is decreased, the **6F** curves each cross their respective **6H** curves, so that now the **6H** homopolymers are more easily dissolved in propane than the **6F** homopolymers. The rapid pressure increase of the **6F** curves suggests that the interchange energy on mixing favors polymer–polymer or solvent–solvent interactions more than polymer–solvent interactions. The steric effect of **6F** forces a change in polymer configuration to accommodate the CF₃ groups that are now more fully accessible to propane but that exacerbate repulsive alkyl fluorocarbon–hydrocarbon interactions.

Figure 6 compares the cloud-point curves for the same polymers in CO₂ and propane. The **6H** homopolymers are much more soluble in propane than in CO₂ because propane has a larger polarizability than CO₂. However, the **6F** homopolymers are more soluble in CO₂ at low temperatures but are more soluble in propane at high temperature. This temperature-dependent behavior is likely due to CO₂–polymer polar interactions that dominate at low temperatures and propane–polymer dispersion interactions that dominate at high temperatures.

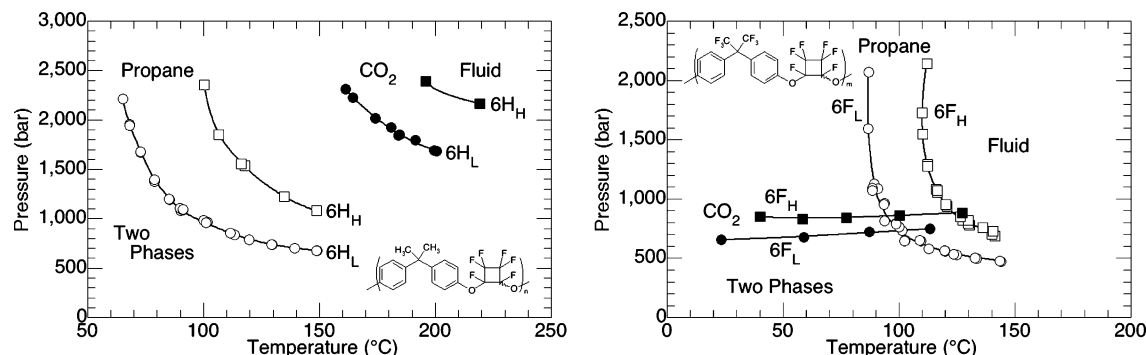


Figure 6. Cloud-point curves for **6H** and **6F** homopolymers in CO₂ and propane: left, **6H** homopolymers; right, **6F** homopolymers.

Conclusions

The phase behavior results reported here demonstrate the significant impact that **6F** has on the phase behavior of rigid backbone polymers in CO₂ and propane, two distinctly different supercritical fluid solvents. Cloud-point data were reported for PFCB copolymers where the **6F** content was changed in a systematic manner. Just adding a relatively modest amount of **6F** to the backbone results in a significant reduction in the cloud-point temperatures and pressures of these polymers in both supercritical CO₂ and propane. With CO₂ as the solvent, the cloud-point curves continually shift to lower temperatures and pressures as the **6F** content is increased. This shift is ascribed to (1) the decrease in long-range, chain–chain interactions due to poor packing of the **6F**-rich chains, (2) the configuration of **6F**-rich chains that exhibit increased solvent accessible surface area of fluorinated groups and, therefore, increase the amount of fluorine–CO₂ polar interactions found with semifluorinated polymers,^{17,21,27,28} and (3) the increase in the fractional free volume of **6F**-rich chains. With propane as the solvent, the cloud-point curves initially shift to lower temperatures and pressures, but the **6F** homopolymer and **6H** homopolymer curves actually cross one another in pressure–temperature space. The **6H** homopolymers are more soluble in propane at low temperatures while **6F** homopolymers are more soluble in propane at high temperatures. This reversal in propane solubility behavior with increasing **6F** content and with temperature results from a delicate balance between unfavorable fluorine–hydrocarbon interactions and favorable reduced long-range, chain–chain interactions and an increase in polymer free volume. Given the large changes in the observed, macroscopic phase behavior for these systems, light scattering studies are in progress to determine whether a significant change in the chain conformation can also be observed.

Acknowledgment. We thank the National Science Foundation (DMR 0514622) and Defense Advanced Research Projects Agency (N66001-03-1-8900) for financial support. D. W. Smith, Jr., is a *Cottrell Scholar of Research Corporation*.

References and Notes

- McHugh, M. A.; Krukonis, V. J. *Supercritical Fluid Extraction: Principles and Practice*, 2nd ed.; Butterworth: Stoneham, 1994.
- Jessop, P. G.; Ikariya, T.; Noyori, R. *Chem. Rev.* **1999**, *99*, 475–493.
- Jessop, P. G.; Leitner, W. *Chemical Synthesis Using Carbon Dioxide*; Wiley/VCH: Weinheim, 1999.
- Kendall, J. L.; Canelas, D. A.; Young, J. L.; DeSimone, J. M. *Chem. Rev.* **1999**, *99*, 543–563.
- Leitner, W. *Acc. Chem. Res.* **2002**, *35*, 746–756.
- Beckman, E. J. *Chem. Commun.* **2004**, 1885–1888.
- Cooper, A. I. *J. Mater. Chem.* **2000**, *10*, 207–234.
- Cooper, A. I. *Adv. Mater.* **2003**, *15*, 1049–1059.
- Woods, H. M.; Silva, M.; Nouvel, C.; Shakesheff, K. M.; Howdle, S. M. *J. Mater. Chem.* **2004**, *14*, 1663–1678.
- Rindfleisch, F.; DiNoia, T. P.; McHugh, M. A. *J. Phys. Chem.* **1996**, *100*, 15581–15587.
- Shen, Z.; McHugh, M. A.; Xu, J.; Belardi, J.; Kilic, S.; Mesiano, A.; Bane, S.; Karnikas, C.; Beckman, E. J.; Enick, R. *Polymer* **2003**, *44*, 1491–1498.
- Yonker, C. R. *J. Phys. Chem. A* **2000**, *104*, 685–691.
- Yonker, C. R.; Palmer, B. J. *J. Phys. Chem. A* **2001**, *105*, 308–314.
- Dardin, A.; DeSimone, J. M.; Samulski, E. T. *J. Phys. Chem. B* **1998**, *102*, 1775–1780.
- Kanakubo, M.; Umecky, T.; Raveendran, P.; Ebina, T.; Ikushima, Y. *J. Solution Chem.* **2004**, *33*, 863–874.
- Temtem, M.; Casimiro, T.; Santos, A. G.; Macedo, A. L.; Cabrita, E. J.; Aguiar-Ricardo, A. *J. Phys. Chem. B* **2007**, *111*, 1318–1326.
- Baradie, B.; Shoichet, M. S.; Shen, Z.; McHugh, M. A.; Hong, L.; Wang, Y.; Johnson, J. K.; Beckman, E. J.; Enick, R. M. *Macromolecules* **2004**, *37*, 7799–7807.
- Costa Gomes, M. F.; Padua, A. A. H. *J. Phys. Chem. B* **2003**, *107*, 14020–14024.
- Cui, S. T.; Cochran, H. D.; Cummings, P. T. *J. Phys. Chem. B* **1999**, *103*, 4485–4491.
- Diep, P.; Jordan, K. D.; Johnson, J. K.; Beckman, E. J. *J. Phys. Chem. A* **1998**, *102*, 2231–2236.
- Fried, J. R.; Hu, N. *Polymer* **2003**, *44*, 4363–4372.
- Galand, N.; Wipff, G. *New J. Chem.* **2003**, *27*, 1319–1325.
- Higashi, H.; Iwai, Y.; Miyazaki, K.; Arai, Y. *Mol. Simul.* **2005**, *31*, 725–730.
- Raveendran, P.; Wallen, S. L. *J. Phys. Chem. B* **2003**, *107*, 1473–1477.
- Stone, M. T.; da Rocha, S. R. P.; Rossky, P. J.; Johnston, K. P. *J. Phys. Chem. B* **2003**, *107*, 10185–10192.
- Stone, M. T.; Smith, P. G.; da Rocha, S. R. P.; Rossky, P. J.; Johnston, K. P. *J. Phys. Chem. B* **2004**, *108*, 1962–1966.
- Kirby, C. F.; McHugh, M. A. *Chem. Rev.* **1999**, *99*, 565–602.
- Mertdogan, C. A.; Byun, H.-S.; McHugh, M. A.; Tuminello, W. H. *Macromolecules* **1996**, *29*, 6548–6555.
- Cassidy, P. E.; Aminabhavi, T. M.; Farley, J. M. *J. Macromol. Sci., Rev. Macromol. Chem. Phys.* **1989**, *C29*, 365–429.
- Cassidy, P. E.; Fitch, J. W., III. Hexafluoroisopropylidene-containing polymers. In *Modern Fluoropolymers: High Performance Polymers for Diverse Applications*; Scheirs, J., Ed.; Wiley: New York, 1997; p 173.
- Smart, B. E. *J. Fluorine Chem.* **2001**, *109*, 3–11.
- Espeso, J.; Lozano, A. E.; de la Campa, J. G.; de Abajo, J. J. *Membr. Sci.* **2006**, *280*, 659–665.
- Shen, Z.; McHugh, M. A.; Smith, D. W. Jr.; Abayasinghe, N. K.; Jin, J. Y. *J. Appl. Polym. Sci.* **2005**, *97*, 1736–1743.
- Smith, D. W., Jr.; Jin, J. Y.; Shah, H. V.; Xie, Y.; DesMarteau, D. D. *Polymer* **2004**, *45*, 5755–5760.
- Spraul, B. K. Aromatic trifluorovinyl ethers: synthesis, characterization and polymerization. Ph.D. Clemson University, Clemson, SC, 2005.
- Tullos, G. L.; Cassidy, P. E.; St Clair, A. K. *Macromolecules* **1991**, *24*, 6059–6064.
- Fodor-Csorba, K.; Vajda, A.; Jakli, A.; Slugovc, C.; Trimmel, G.; Demus, D.; Gacs-Baitz, E.; Holly, S.; Galli, G. *J. Mater. Chem.* **2004**, *14*, 2499–2506.
- Shimazu, A.; Miyazaki, T.; Maeda, M.; Ikeda, K. *J. Polym. Sci., Part B: Polym. Phys.* **2000**, *38*, 2525–2536.
- Dunitz, J. D.; Gavezzotti, A.; Schweizer, W. B. *Helv. Chim. Acta* **2003**, *86*, 4073–4092.
- Gaudiana, R. A.; Minns, R. A.; Sinta, R.; Weeks, N.; Rogers, H. G. *Prog. Polym. Sci.* **1989**, *14*, 47–89.
- Liu, B. J.; Hu, W.; Chen, C. H.; Jiang, Z. H.; Zhang, W. J.; Wu, Z. W. *Polym. Adv. Technol.* **2003**, *14*, 221–225.
- Grob, M. C.; Feiring, A. E.; Auman, B. C.; Percec, V.; Zhao, M. Y.; Hill, D. H. *Macromolecules* **1996**, *29*, 7284–7293.

MA070515B